

A burst-feedback model of fast-phase burst generation during nystagmus

Thomas J. Anastasio

Beckman Institute and Department of Molecular and Integrative Physiology, University of Illinois at Urbana/Champaign, Urbana, Illinois, USA

Received: 11 April 1996 / Accepted in revised form: 6 August 1996

Abstract. Vestibular and optokinetic nystagmus are characterized by alternating slow-phase eye rotations that stabilize the retinal image, and fast-phase eye rotations that reset eye position. Nystagmus is coordinated in the brainstem by burst neurons that fire an intense, temporally circumscribed burst that terminates the slow phase and drives the fast phase. This paper demonstrates that such a burst can be generated during nystagmus using a simple neural network model containing only known brainstem neurons and their interconnections. These include the feedback connections of the burst neuron (burst feedback). The burst neuron excites itself directly, and disinhibits itself by inhibiting the pause neuron (positive feedback). It also inhibits itself by inhibiting the vestibular neuron (negative feedback). The burst neuron begins to fire after its inhibitory bias is overcome by excitation from the vestibular neuron, and burst neuron positive feedback then produces an intense burst with an abrupt onset. The burst causes the vestibular and pause neurons to pause. The benefit of the pause neuron loop is that it contributes to burst neuron positive feedback when it is needed at burst onset, but that contribution is eliminated when the pause neuron pauses and opens the loop. The burst can then terminate, with an offset duration proportional to burst amplitude, under the control of burst neuron self-excitation and inhibitory bias. Model neuron behavior is comparable to that of real brainstem neurons. Synchronized bursts can be produced over the population of burst neurons in a distributed version of the network. Variability in connection weights in the distributed network results in variability in prelude activity among burst neurons that is similar to the spread in lead observed for real burst neurons during nystagmus.

1 Introduction

Stabilization of the retinal image during movement is accomplished by the concerted actions of the vestibular and optokinetic systems (Robinson 1989). The vestibular system uses head velocity information to produce eye rotations that oppose head rotations, while the optokinetic system uses information about the velocity of the visual world to match the rotations of the eye to those of the surroundings. These relatively slow, stabilizing eye rotations are kept within bounds by fast eye rotations that reset eye position. The alteration of slow-phase and fast-phase eye rotations constitutes vestibular and optokinetic nystagmus. Single-unit recordings from the brainstem indicate that nystagmus is coordinated by burst neurons which fire an intense, temporally circumscribed burst that terminates the slow phase and drives the fast phase (Hikosaka et al. 1977; Curthoys et al. 1981; Markham et al. 1981). The burst has the following characteristics: it can occur during nystagmus driven by a constant input, it has an abrupt onset, it has a large amplitude (up to 1000 spikes/s), and it has a rapid offset. Also, the burst is synchronized over an entire population of burst neurons, and low-intensity prelude activity is observed for some burst neurons but not others.

The burst neurons that drive fast phases during nystagmus are the same as those that drive goal-directed saccades (Keller 1974). For this reason, previous nystagmus models have treated fast phases as saccades, and have included the circuitry for making saccadic bursts as part of their structure (Schmidt and Lardini 1976; Chun and Robinson 1978). However, later studies revealed that fast phases are spared by lesions of the superior colliculus and frontal eye fields that eliminate goal-directed saccades (Schiller et al. 1980; Albano and Wurtz 1982). A more recent model of nystagmus left out the saccadic circuitry, and simply controlled burst onset and offset with a switch (Galiana 1991). In all previous nystagmus models the fast-phase burst is controlled, at least in part, by 'blackboxes.' Thus, previous models leave open the question of how an intense, temporally circumscribed burst can be generated during nystagmus by a real neural circuit confined to the brainstem. Also, since the previous

Correspondence ψ to: T. J. Anastasio, Ph.D., University of Illinois, Beckman Institute, 405 North Mathews Ave., Urbana, IL 61801, USA (Fax: +1(217)-244-5180; e-mail: tstasio@uiuc.edu)

nystagmus models are not distributed, they cannot explain the variability in prelude activity, and subsequent burst synchrony, that is observed over the burst neuron population.

In a model of the saccadic burst generator, Scudder (1988) proposed a neural circuit that employs feedback from the burst neurons to control the dynamics of bursts driven by the superior colliculus. In that model, burst neurons exert positive and negative feedback on themselves both directly and indirectly. The saccadic burst-feedback model is composed almost entirely of known brainstem neurons and their interconnections. However, it cannot be used to generate fast-phase bursts without a burst input from the superior colliculus.

The purpose of this paper is to propose a model of the fast-phase burst generator that will produce an intense, temporally circumscribed burst during nystagmus using only known brainstem neurons and their interconnections. Variability in prelude activity, and subsequent burst synchrony over a population of burst neurons, will be demonstrated in a distributed version of the model. The fast-phase burst-feedback model described here is a modification of the saccadic burst-feedback model (Scudder 1988). The function of the fast-phase burst-feedback model will be developed analytically, and simulations from the model will be compared with data on brainstem premotor neurons collected primarily during nystagmus, but also during saccades. Because saccadic eye-movement metrics are encoded by the temporal discharge characteristics of burst neurons (Kaneko et al. 1981; Yoshida et al. 1982; Scudder et al. 1988), the same will be assumed for fast-phase eye movements. However, the focus of the model is on burst generation by burst neurons. The details of fast-phase and slow-phase eye movements are beyond its focus.

2 Model architecture

The fast-phase burst-feedback model is a neural network, the structure of which is based on the real brainstem premotor network that mediates nystagmus. To focus attention on fast-phase burst generation, the model is a unilateral simplification of the bilateral brainstem network. A schematic of the model is shown in Fig. 1. Brainstem neurons that mediate nystagmus include vestibular nucleus, burst, and pause neurons (Shimazu 1983). These neurons are represented in the model by units labeled with pairs of upper-case letters: vestibular nucleus (*VN*), burst neuron (*BN*), and pause neuron (*PN*). Additionally, a unit representing an input neuron (*IN*) carries constant, vestibular or optokinetic inputs, and a bias or 'on' neuron (*ON*) carries a constant, nonspecific input. Connections between the units are designated by pairs of lower-case letters, where the first and second letters in the pair label the post- and presynaptic unit, respectively (to/from). For example, the connection to *BN* from *VN* is labeled *bv*. Likewise, the connection to *BN* from itself is *bb*. Excitatory and inhibitory connections are shown as open and filled arrows, respectively. Labels for the units and their connections are given in Table 1A. The abso-

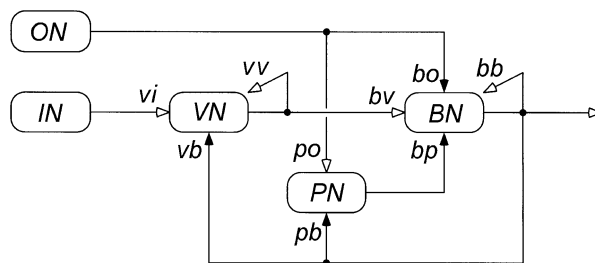


Fig. 1. Burst-feedback neural network model of fast-phase burst generation. Each unit is labeled by a pair of upper-case letters: *ON*, bias or 'on' neuron; *IN*, input neuron; *VN*, vestibular nucleus neuron; *BN*, burst neuron; *PN*, pause neuron. Unit *ON* has a constant value of 1 in all simulations. Pairs of lower-case letters label the connections between the units in the network. The first and second lower-case letters in a pair designate the post- and presynaptic model neuron, respectively (to/from): *vi*, to *VN* from *IN*; *vb*, to *VN* from *BN*; *vv*, to *VN* from *VN*; *bv*, to *BN* from *VN*; *bo*, to *BN* from *ON*; *bp*, to *BN* from *PN*; *bb*, to *BN* from *BN*; *po*, to *PN* from *ON*; *pb*, to *PN* from *BN*. Excitatory and inhibitory connections are shown as open arrows and filled arrows, respectively. Connection labels and weights are given in Table 1

Table 1. Connection weight matrices for the burst-feedback neural network model of fast-phase burst generation

Connection to	Connection from				
	<i>ON</i>	<i>IN</i>	<i>VN</i>	<i>BN</i>	<i>PN</i>
A: Connections between the units in the network					
<i>VN</i>	<i>vo</i>	<i>vi</i>	<i>vv</i>	<i>vb</i>	<i>vp</i>
<i>BN</i>	<i>bo</i>	<i>bi</i>	<i>bv</i>	<i>bb</i>	<i>bp</i>
<i>PN</i>	<i>po</i>	<i>pi</i>	<i>pv</i>	<i>pb</i>	<i>pp</i>
B: Connection weights for the network <i>without PN</i>					
<i>VN</i>	0	1	1	-1	0
<i>BN</i>	-20	0	1	1	0
<i>PN</i>	0	0	0	0	0
C: Connection weights for the network <i>with PN</i>					
<i>VN</i>	0	1	1	-1	0
<i>BN</i>	-10	0	3	1	-10
<i>PN</i>	5	0	0	-1	0

Pairs of upper-case letters label the units in the network which model the following types of neurons: *ON*, bias or 'on' neuron; *IN*, input neuron; *VN*, vestibular nucleus neuron; *BN*, burst neuron; *PN*, pause neuron. Pairs of lower-case letters label the connections between the units in the network. The first and second lower-case letters in a pair designate the post- and presynaptic model neuron, respectively (to/from). For example, *bv* labels the connection to *BN* from *VN*, and *bb* labels the connection to *BN* from itself

lute values of the connections are varied for the purposes of analysis and simulation (e.g. Table 1B, C). A distributed version of the fast-phase burst-feedback network has the same structure as the lumped version (Fig. 1) but has 10 each of *VN*, *BN*, and *PN*.

The connections in the network are based upon neuro-anatomical and neurophysiological evidence, primarily from cats and monkeys. Vestibular nucleus neurons integrate the vestibular and optokinetic velocity inputs they receive, to produce the eye-position commands that drive

the slow phase of nystagmus (Robinson 1989). This neural integration is thought to occur by vestibular neuron self-excitation through other neurons. Burst neurons, that drive the fast phase, can be driven by vestibular neurons either directly (McCrea et al. 1987) or indirectly through relay neurons in the nucleus prepositus and adjacent reticular formation (Okhi et al. 1988).

Burst neurons form two groups that make either excitatory or inhibitory connections with other neurons (Shimazu 1983). Pause neurons project to both types of burst neurons and strongly inhibit them (Keller 1974; Nakao et al. 1980; Langer and Kaneko 1983; Curthoys et al. 1984; Strassman et al. 1987). Inhibitory burst neurons project to pause neurons (King et al. 1980; Ito et al. 1984; Langer and Kaneko 1984). Excitatory burst neurons can also inhibit pause neurons, and can inhibit vestibular nucleus neurons, through inhibitory interneurons (King et al. 1980; Sasaki and Shimazu 1981; Ito et al. 1984, 1986; Strassman et al. 1986a, b). Excitatory burst neurons can excite themselves, either directly or through interneurons in the reticular formation (Strassman et al. 1986a, b). Additionally, excitatory burst neurons excite inhibitory burst neurons (Sasaki and Shimazu 1981; Strassman et al. 1986a, b). Because excitatory and inhibitory burst neurons are functionally coupled, they are combined in the model into a single burst neuron unit that can make both excitatory and inhibitory connections. Pause neurons receive a nonspecific input that endows them with an excitatory bias (Evinger et al. 1977, 1982; Keller 1977). A similar nonspecific source is assumed for burst neuron inhibitory bias. The brainstem connections, simplified by removing interneurons and relay neurons, are represented in the model (Fig. 1).

The model will be used to demonstrate how an intense, temporally circumscribed burst can be generated during nystagmus, driven by a constant input, using only the brainstem neurons and connections represented in it. Fast-phase burst generation in the network is achieved through its feedback connections, principally those of the burst neuron (burst feedback). Because several different feedback pathways are involved, analysis and simulation of the fast-phase burst-feedback network proceeds in stages, which are outlined briefly below before being considered in detail.

The slow-phase stage occurs before the burst when the vestibular neuron is integrating its input. This integration is brought about by positive feedback due to vestibular neuron self-excitation. The burst stage begins after vestibular neuron excitation of the burst neuron overcomes its inhibitory bias and brings the burst neuron to threshold. Two positive feedback loops ensure that the burst will have an abrupt onset and large amplitude. Positive feedback due to burst neuron self-excitation is considered first. Burst neuron self-excitation can be used to generate small bursts only. Realistically large bursts cannot be generated because, if burst neuron self-excitation is too large, the burst cannot be terminated once it is initiated. This limitation is overcome by positive feedback through the pause neuron loop, which is considered next. Because the pause neuron inhibits the burst neuron, the burst neuron exerts positive feedback on itself when it

inhibits the pause neuron. The benefit of the pause neuron loop is that it contributes to burst neuron positive feedback when it is needed at burst onset, but this contribution is eliminated when the pause neuron pauses and opens the loop. The burst-offset stage begins when the vestibular and pause neurons both pause due to burst neuron inhibition. Burst neuron inhibitory bias can terminate the burst during this stage, provided that burst neuron self-excitation is not too large. Both linear and nonlinear versions of the fast-phase burst-feedback network are examined at each stage. A simulation of a distributed version of the fast-phase burst-feedback network is also described.

3 Analysis and simulation

The units in the fast-phase burst-feedback network compute the weighted sum of their inputs. The states of the units are bounded between 0 and 50 in nonlinear versions of the network, but are unbounded in linear versions. Multiplication by 20 spikes/s (sp/s) converts the raw unit states to their equivalent in firing rate. To account for both synaptic and membrane delays, each time step of the model is equivalent to 5 ms. In order to simplify the analysis, the units have no explicit time constant. Without unit time constants, a connection weight of 1 indicates that the presynaptic unit transfers its state in whole to the postsynaptic unit in 1 time step (5 ms). Including unit time constants would alter this simple, easily interpreted arrangement. In any case, the general dynamics of the network are not changed if, for example, the units are given a 10 ms time constant and the time step is reduced to 1 ms.

The dynamics of the fast-phase burst-feedback model are discrete in time. Discrete rather than continuous dynamics are used because the connection weight values in the discrete network are easily interpreted, and because it facilitates comparisons with the saccadic burst-feedback model which is also discrete (Scudder 1988). Mathematically, discrete systems and difference equations are analogous to continuous systems and differential equations (Luenberger 1979). Therefore, insights developed in the discrete case are applicable in the continuous case.

If $k = 0, 1, 2, \dots$ represents discrete, equally spaced time points, then a difference equation relates the value of the function $Y(k)$, at point k , to values at other points. Difference equations can be used to describe the dynamics of discrete systems, and if the difference equations are linear they can be solved using the z -transform (Luenberger 1979). The z -transform $\bar{Y}(z)$ of the discrete function $Y(k)$ is defined as:

$$\bar{Y}(z) = \sum_{k=0}^{\infty} \frac{Y(k)}{z^k} \quad (1)$$

Equation (1) can be used to derive z -transform pairs. For example, if $Y(k)$ has the z -transform $\bar{Y}(z)$, then $Y(k+1)$ has the z -transform $[z \cdot \bar{Y}(z) - z \cdot Y(0)]$ where $Y(0)$ is the initial condition of $Y(k)$. Other useful z -transform

pairs include the following: if $Y(k) = k$ then $\bar{Y}(z) = [z/(z-1)^2]$, if $Y(k) = a^k$ then $\bar{Y}(z) = [z/(z-a)]$, and if $Y(k) = a^{k-1}$ (but $Y(0) = 0$) then $\bar{Y}(z) = [1/(z-a)]$. The z -transforms can be manipulated algebraically, and the solutions of the associated difference equations can be found by the reverse z -transform. Thus, the z -transform for discrete systems is analogous to the Laplace transform for continuous systems (e.g., $\bar{Y}(s) = \int_0^\infty Y(t) \cdot e^{-st} dt$).

3.1 Linear analysis of vestibular nucleus neuron dynamics during the slow phase

To analyze the network before the burst, the burst, pause, and 'on' neurons in the model (BN , PN , and ON , respectively) can be disregarded, and the difference equation can be considered that describes only the dynamics of the vestibular nucleus neuron (VN), which excites itself through positive feedback and is excited by the input neuron (IN):

$$VN(k+1) = vv \cdot VN(k) + vi \cdot IN(k) \quad (2)$$

Equation (2) specifies that the state of VN at time step $k+1$ is equal to the sum of its weighted inputs from itself and from IN at time step k . Because it is linear (i.e., unit states are unbounded), the z -transform of (2) can be taken:

$$z \cdot \bar{VN}(z) - z \cdot VN(0) = vv \cdot \bar{VN}(z) + vi \cdot \bar{IN}(z) \quad (3)$$

Assuming that the initial condition of VN is equal to 0 ($VN(0) = 0$), then the transfer function relating the z -transforms of VN and IN can be written:

$$\frac{\bar{VN}(z)}{\bar{IN}(z)} = \frac{vi}{z - vv} \quad (4)$$

A qualitative appreciation of the dynamics of VN can be obtained by finding the impulse response of (4). This is done by representing the input as the z -transform of the unit impulse, which is simply 1 ($\bar{IN}(z) = 1$), and finding the reverse z -transform:

$$VN(k) = vi \cdot vv^{k-1} \quad (5)$$

Equation (5) indicates that VN will be a perfect integrator if the value of its self-connection vv is equal to 1, since then VN for all k will be a step of size vi , which is the size of the weighted impulse it received as its input. Equation (5) also indicates that for $0 < vv < 1$, VN will be stable and its impulse response will decay to 0 geometrically, but for $vv > 1$, VN will be unstable and its impulse response will grow to infinity geometrically. Geometric growth and decay are the discrete analogs of exponential growth and decay in continuous systems. (The impulse response of VN for $vv < 0$ would be an alternating sequence of positive and negative values, but this type of response is not considered here.) Equation (5) gives the discrete impulse response of VN exactly. However, the same qualitative appreciation of the dynamics of VN could have been obtained by noting that vv is the eigenvalue of the homogeneous part of (2), which de-

scribes the free (i.e., undriven by the input), linear dynamics of the VN system (Luenberger 1979).

Recall that for $vv > 1$, VN will be unstable. The analysis underscores the fact that systems with positive feedback are prone to instability. In the complete fast-phase burst-feedback network (Fig. 1) there are two additional positive feedback loops, both onto the burst neuron (BN). BN exerts positive feedback on itself directly with an excitatory self-connection (bb). Because the pause neuron (PN) inhibits BN , BN disinhibits itself by inhibiting PN , and this also amounts to positive feedback. VN excites BN , and even though BN exerts negative feedback on itself by inhibiting VN , the network is unlikely to be stable. An analysis is necessary to determine whether and under what circumstances the fast-phase burst-feedback network can generate bursts.

3.2 Analysis of the linear fast-phase burst-feedback network without the pause neuron

In order to determine the underlying dynamics of the fast-phase burst-feedback network, it is necessary to consider the system in the absence of PN . The equation for the linear (i.e., unbounded) system *without* PN can be written in matrix notation as:

$$\begin{bmatrix} BN(k+1) \\ VN(k+1) \end{bmatrix} = \begin{bmatrix} bb & bv \\ vb & vv \end{bmatrix} \cdot \begin{bmatrix} BN(k) \\ VN(k) \end{bmatrix} + \begin{bmatrix} bo & 0 \\ 0 & vi \end{bmatrix} \cdot \begin{bmatrix} ON(k) \\ IN(k) \end{bmatrix} \quad (6)$$

Equation (6) specifies that the state of BN at time step $k+1$ is equal to the sum of its weighted inputs from itself, VN , and ON at time step k , and that the state of VN at time step $k+1$ is equal to the sum of its weighted inputs from itself, BN , and IN at time step k . The exact solution of (6) by z -transforms is cumbersome. However, the general form of the response can be determined from the eigenvalues of the matrix of the homogeneous (i.e., undriven or free) system (Luenberger 1979). The system matrix \mathbf{A} is:

$$\mathbf{A} = \begin{bmatrix} bb & bv \\ vb & vv \end{bmatrix} \quad (7)$$

The elements of system matrix \mathbf{A} are the weights of the connections of BN and VN to themselves and to each other. The eigenvalues of the system can be found by solving its characteristic equation for λ :

$$\det[\mathbf{A} - \lambda \mathbf{I}] = (bb - \lambda) \cdot (vv - \lambda) - (bv \cdot vb) = 0 \quad (8)$$

where \mathbf{I} is the identity matrix and \det represents the determinant. Because the characteristic equation (8) is quadratic, the fast-phase burst-feedback network *without* PN will have two eigenvalues ($\lambda_{1,2}$) for each configuration (i.e., set of weights). Using the quadratic formula, this pair of eigenvalues is found to be:

$$\lambda_{1,2} = \frac{(bb + vv) \pm \sqrt{(bb - vv)^2 + 4 \cdot (bv \cdot vb)}}{2} \quad (9)$$

Equation (9) is used to calculate the eigenvalues ($\lambda_{1,2}$) of the fast-phase burst-feedback network *without* PN .

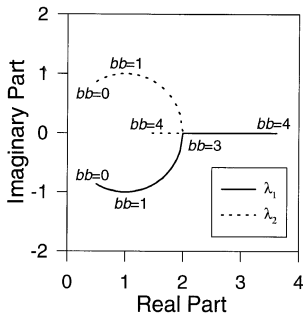


Fig. 2. Eigenvalues of the linear fast-phase burst-feedback network *without* the pause neuron. Connection weights are given in Table 1B, except for the connection to the burst neuron from itself (bb), which is varied from 0 to 4. The eigenvalues (λ_1 , continuous line; λ_2 , dotted line) are plotted on real and imaginary axes (i.e., in the complex plane). The eigenvalue pairs are complex conjugates for $0 \leq bb < 3$, real and repeated for $bb = 3$, and real and distinct for $bb > 3$

Because VN should be a perfect integrator the value of vv is set to 1. For simplicity, the values of bv and vb are set to 1 and -1 , respectively. To determine the effects of changes in BN self-excitation on model dynamics, the value of bb is varied from 0 to 4 while the other weights are held constant. The eigenvalues are calculated (9) and are plotted in Fig. 2 in the complex plane (λ_1 , continuous line; λ_2 , dotted line).

For the fast-phase burst-feedback network *without* PN , the pair of eigenvalues are complex conjugates for $0 \leq bb < 3$, real and repeated for $bb = 3$, and real and distinct for $bb > 3$. Each eigenvalue has associated with it a magnitude and an angle in the complex plane. For discrete linear systems, the magnitude and angle indicate, respectively, the rate of geometric growth (or decay) and the frequency of oscillation of the response due to that eigenvalue (Luenberger 1979). The angle is non-zero only for complex eigenvalues. Therefore, the response of the fast-phase burst-feedback network *without* PN will be oscillatory for $0 \leq bb < 3$, and nonoscillatory for $bb \geq 3$. The angle, and thus the frequency of oscillation, decreases as the value of bb increases, and the oscillation frequency is highest when $bb = 0$. At any time step k , the size (or amplitude) of the response of a discrete linear system is related to the magnitude of the largest eigenvalue raised to the power k . For the model *without* PN , the magnitude of the eigenvalues (or of the larger eigenvalue in a pair of real and distinct eigenvalues) is 1 for $bb = 0$, and increases above 1 as bb increases above 0. Therefore, the response will be marginally stable (i.e., maintain a constant amplitude) for $bb = 0$, but will be unstable (i.e., grow geometrically) for $bb > 0$. The responses of the linear network can be illustrated through simulations.

3.3 Simulations of the linear fast-phase burst-feedback network *without* the pause neuron

The responses of BN in the linear fast-phase burst-feedback network *without* PN are illustrated in Fig. 3 for

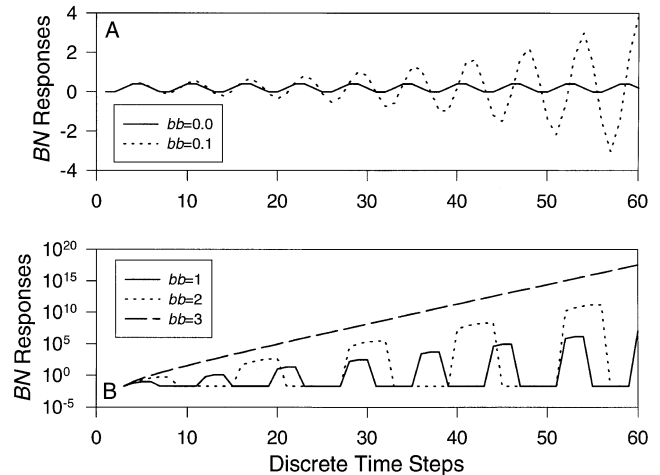


Fig. 3A, B. Burst neuron responses in the linear fast-phase burst-feedback network *without* pause neurons. Unit states are unbounded. Connection weights are given in Table 1B, except for the connection from the burst neuron to itself (bb), which is varied as shown. **A** bb takes the values of 0.0 and 0.1 (continuous and dotted lines, respectively). **B** bb takes the values of 1, 2, and 3 (continuous, dotted, and dashed lines, respectively). The burst neuron response oscillates with a constant amplitude for $bb = 0$, oscillates with a geometrically increasing amplitude for $bb = 0.1, 1$, and 2 , and rises geometrically without oscillating for $bb = 3$. For the semilogarithmic plots in **B**, 0 and negative values have been removed

various values of bb (BN self-excitation). The values of the other weights used in these simulations are given in Table 1B. This network configuration is the one used for simulations of the nonlinear network *without* PN described below. For example, BN receives an inhibitory connection of 20 from ON ($bo = -20$), which represents the burst threshold for the nonlinear network. VN has an initial state of 20, so that BN will have a positive initial response. Also, the network receives a constant input of 0.2 (i.e., the state of IN is held constant at 0.2). Providing an initial condition and an input will affect the responses quantitatively but not qualitatively (Luenberger 1979).

For $bb = 0$, the response of BN in the linear fast-phase burst-feedback network *without* PN is oscillatory and has a constant amplitude (Fig. 3A, continuous line). For $bb = 0.1$ (Fig. 3A, dotted line) the response is also oscillatory but has an amplitude that grows geometrically as k increases. Semilogarithmic plots of the unstable oscillatory responses have amplitude envelopes that increase linearly with k , as shown for $bb = 1$ and $bb = 2$ (Fig. 3B, continuous and dotted lines, respectively). [For the semilogarithmic plots (Fig. 3B), 0 and negative values have been removed.] The oscillation has a lower frequency but more rapidly growing amplitude for $bb = 2$ than for $bb = 1$. The response of BN increases rapidly but is nonoscillatory for $bb = 3$ (Fig. 3B, dashed line). The analysis and simulations show that the linear fast-phase burst-feedback network *without* PN is unstable. However, as explained below, the nonlinear (i.e., bounded) network can generate fast-phase bursts provided that the linear response is oscillatory ($0 \leq bb < 3$).

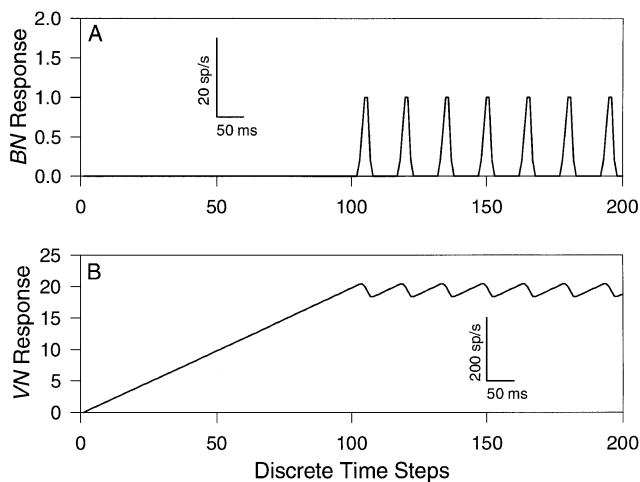


Fig. 4A, B. Neural responses in the nonlinear fast-phase burst-feedback network *without* pause neurons. Unit states are bounded between 0 and 50. Connection weights are given in Table 1B; the burst neuron self-connection bb has the value of 1. The burst neuron (BN , shown in **A**) produces a series of bursts after its input from the vestibular neuron (VN , shown in **B**) brings it to threshold. The BN bursts represent the first positive half-cycle of the unstable oscillation shown as a *continuous line* in Fig. 3B ($bb = 1$). However, these bursts are small and unable to produce a complete pause in VN . The axes show the discrete time steps and actual values of the unit states, while the *scale bars* provide a gauge for comparison with neurophysiological data. This convention is followed in subsequent figures

3.4 Simulations of the nonlinear fast-phase burst-feedback network *without* the pause neuron

Fast-phase bursts are generated using the nonlinear network *without PN* to try to simulate the pattern of activity observed for real burst and vestibular nucleus neurons during nystagmus. To simulate nystagmus a constant input of 0.2 is provided to VN from IN . The units are nonlinear (states are bounded between 0 and 50), and the network is configured with the weights given in Table 1B. These include an inhibitory connection to BN from ON of 20 ($bo = -20$). This represents the threshold of the burst generator because, in the nonlinear (bounded) case, BN cannot begin to fire until its excitatory input from VN exceeds its inhibitory input from ON (constant inhibitory bias) and its state becomes positive. A threshold of 20 is chosen because this corresponds to the approximately 400 sp/s firing rate attained by real vestibular nucleus neurons before burst onset (Hikosaka et al. 1977; Curthoys et al. 1981; Markham et al. 1981).

VN integrates its constant input and produces a ramp with which it excites BN . When the excitation from VN exceeds the inhibition from ON , BN begins to fire. With VN and BN both firing in the linear range (between 0 and 50) the linear dynamics of the network described above become engaged. If the weight of BN self-excitation is 3 or greater ($bb \geq 3$), then the state of BN will begin to grow geometrically until it reaches the upper bound at 50, and there it will remain even if it fully inhibits VN and thereby cuts off its external drive. How-

ever, if $0 \leq bb < 3$, then the state of BN will begin to oscillate. Importantly, because unit states in the nonlinear network have a lower bound at 0, BN will only oscillate for the first positive half-cycle, after which BN will cut off, the linear dynamics will become disengaged, and the oscillation will cease. If the frequency of the oscillation is high, then the first positive half-cycle will resemble a burst.

Burst generation in the nonlinear fast-phase network *without PN* is illustrated in Fig. 4. Network connections are given in Table 1B with $bb = 1$. When the VN ramp (Fig. 4B) exceeds the BN threshold (20), BN begins to fire (Fig. 4A). At that point the linear dynamics are engaged, and the response of BN is the first positive half-cycle of the unstable oscillation shown in Fig. 3B for $bb = 1$ (continuous line). Because BN inhibits VN ($vb = -1$), the burst in BN produces a small dip in VN firing rate. After the dip, VN ramps back up to the BN threshold, another BN burst is initiated, and the process is repeated.

Discrepancies between simulated and observed neural firing patterns are apparent. The axes in Fig. 4 (and other figures) represent the actual values of the discrete time steps and unit states. They are scaled to 5 ms and 20 sp/s per unit of time and state in the network, respectively, and the scale bars in the figures are provided as a gauge. The bursts from the nonlinear network *without PN* (Fig. 4A) are about 30 ms in duration. That duration is at the short end of the range of burst durations observed during nystagmus (Curthoys et al. 1981; Markham et al. 1981). However, the burst amplitude of 20 sp/s is many times smaller than the 400–800 sp/s that has been observed during nystagmus (Curthoys et al. 1981; Markham et al. 1981). This small burst is unable to produce a complete pause in VN (Fig. 4B). Burst amplitude in the fast-phase burst-feedback network *without PN* is unrealistically small.

Burst amplitude can be increased by increasing the absolute values of the feedback connection weights in the fast-phase network *without PN*, but this has undesirable consequences. For example, burst amplitude can be increased by increasing VN self-excitation vv , but this is undesirable because it causes the VN integrator to become unstable. Burst amplitude can also be increased by increasing BN self-excitation bb . As noted above in the linear analysis and simulations, the amplitude envelope of the unstable oscillation increases, but the frequency decreases, as bb increases from 0 to 3. Desired characteristics for a burst include a large amplitude and a sharp onset. While increasing the value of bb increases the amplitude envelope of the unstable oscillation, it also decreases the frequency, and this dulls the onset of the burst. For example, with the configuration given in Table 1B, doubling the value of bb (from 1 to 2) only increases burst amplitude from 20 sp/s to 112 sp/s, while the time to peak is almost doubled. Other undesirable consequences of increasing BN self-excitation will be presented below.

Equation (9) shows that the imaginary part of the complex eigenvalues increases with the absolute values of the weights connecting VN and BN (bv and vb ; note that vb is negative). This would increase both the magnitude

and the angle of the eigenvalues, indicating increases in both the amplitude envelope and the frequency of the unstable oscillation. However, increasing the frequency would decrease the duration of an already short burst. Also, although increasing bv and/or vb increases the amplitude envelope, it does not necessarily increase the amplitude of the first positive half-cycle because the higher frequency could cause the oscillation to move to negative values sooner. For example, doubling the absolute value of the inhibitory connection to VN from BN (vb) actually decreases both the duration and the amplitude of the burst. In contrast, large increases in the excitatory connection to BN from VN (bv) can produce large increases in burst amplitude. For example, bursts of 800 sp/s can be produced by increasing bv to 80. However, burst duration is only about 15 ms, which is unrealistically short. Also, the weight of the inhibitory connection to BN from ON has to be increased by 80 times ($bo = -1600$) to keep the threshold of the burst generator at 20, and this seems unrealistically high.

Burst generation in the network *without* PN has other unrealistic characteristics. These include a strong dependency of burst amplitude on input size. The input IN represents the drive to the fast-phase burst generator and would be proportional to the velocity of the slow-phase of nystagmus. For the network configured with the weights given in Table 1B, burst amplitudes for constant inputs (IN states) of 0.002, 0.02, 0.2, and 2.0 are respectively 0.2, 2, 20, and 200 sp/s. These data show that burst amplitude scales directly with input size. This is expected for a linear system, such as the network *without* PN during the period of the burst when BN and VN are both on. In contrast, for the network *without* PN , burst duration is independent of input size because the input merely scales the burst. These features are unrealistic since fast-phase duration decreases as the slow-phase velocity of nystagmus increases while fast-phase amplitude during nystagmus is largely independent of slow-phase velocity (Honrubia et al. 1971a, b).

In summary, the nonlinear burst-feedback network *without* PN can generate fast-phase bursts. These bursts are the first positive half-cycle of an unstable oscillation that is engaged and disengaged as BN cuts on and off. In the network *without* PN , however, bursts with a realistically large amplitude cannot be generated unless unrealistic modeling assumptions are made. Also, burst amplitude is dependent on input size, while burst duration is independent of input size in the network *without* PN , and that is unrealistic. It is clear that this mechanism, in which a burst is generated as the first positive half-cycle of an unstable oscillation involving BN and VN , cannot alone account for real fast-phase burst generation during nystagmus.

3.5 Simulations of the nonlinear fast-phase burst-feedback network with the pause neuron

Including PN in the network eliminates the unrealistic features of burst generation. To simulate burst generation *with* PN , the network is configured with the weights given in Table 1C. PN receives an excitatory connection

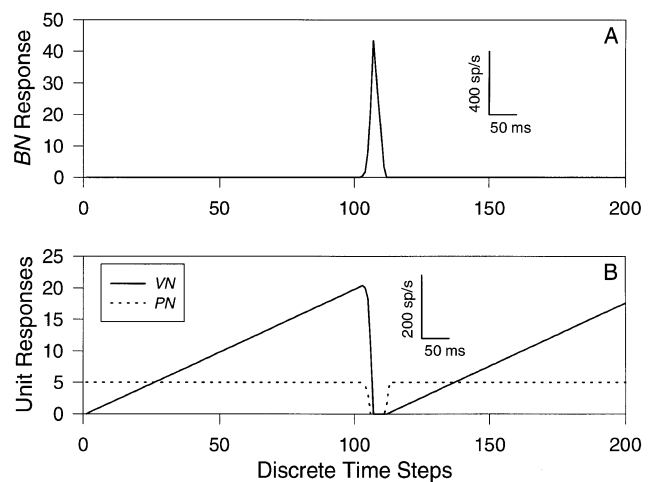


Fig. 5A, B. Neural responses in the nonlinear fast-phase burst-feedback network *with* pause neurons. Unit states are bounded. Connection weights are given in Table 1C; the burst neuron self-connection bb has the value of 1. The burst neuron (BN) produces an intense burst (**A**), and this burst is sufficient to produce a complete pause in both the vestibular and pause neurons (**B**; VN , continuous line; PN , dotted line)

from ON with a weight of 5 ($po = 5$). This endows PN with a constant firing rate of 100 sp/s, which is typical for real pause neurons (Luschei and Fuchs 1972; Evinger et al. 1977, 1982). PN inhibits BN with a connection weight of 10 ($bp = -10$). BN in turn inhibits PN with a connection weight of 1 ($pb = -1$). With PN included, bo is changed to -10 from -20 . With the constant states of ON and PN at 1 and 5, respectively, and both inhibiting BN by 10, the total inhibition of BN is 60. To keep the threshold at 20, the value of the excitatory connection to BN from VN is increased to 3 ($bv = 3$, Table 1C). This increase in bv contributes virtually nothing to burst size by itself because, in the network *without* PN , it increases burst amplitude to only 36 sp/s and decreases burst duration by almost half.

Burst generation in the nonlinear fast-phase network *with* PN is illustrated in Fig. 5. Network connections are given in Table 1C. The input (IN) is constant at 0.2. As in the network *without* PN , BN fires a burst (Fig. 5A) after it is brought to threshold by the VN ramp (Fig. 5B). However, the network *with* PN produces an intense burst, with an amplitude of 868 sp/s, that is strong enough to produce a complete pause in the activity of both VN and PN . The pattern of behavior shown for BN , VN , and PN is similar to that observed for real burst, vestibular nucleus, and pause neurons during nystagmus (Hikosaka et al. 1977; Curthoys et al. 1981; Markham et al. 1981; see Sect. 4).

In the network *with* PN , BN inhibits PN and PN inhibits BN in turn. Thus, BN disinhibits itself when it fires by inhibiting PN . This forms a positive feedback loop onto BN , in addition to the loop formed by direct BN self-excitation. Just after BN begins to fire, during the

brief period when BN , VN , and PN are all firing, the effect of the PN loop is to increase the amount of BN positive feedback, in effect increasing the value of the BN self-excitation weight (bb). The analysis of the linear network *without* PN shows that increasing the value of bb can cause the dynamics of the network to change from an unstable oscillation to unstable geometric growth (Fig. 3B).

With the configuration for the network *with* PN given in Table 1C, the effective increase in bb brought about by the PN loop is such that the linear dynamics change to unstable geometric growth. In the network *without* PN , nonoscillatory dynamics could produce rapid geometric growth in the state of BN , but could not produce a burst, because the state of BN would never return to 0. However, in the network *with* PN , the extra positive feedback due to the PN loop, which endows BN with rapid geometric growth at burst onset, is eliminated as soon as PN cuts off (see Sect. 3.8). The large BN burst produces a complete pause in both PN and VN , and this leaves BN in isolation from the rest of the network, except for its self-excitation and inhibition from ON . Under certain circumstances (see below), inhibition from ON will allow the state of BN to return to 0 after both PN and VN cut off. Thus, in the network *with* PN , high positive feedback can be produced at burst onset, and then switched off to allow the state of BN to return to 0 again.

3.6 Linear analysis of burst offset in the burst-feedback network with the pause neuron

After the peak of the burst, with VN and PN both off, BN is isolated from the rest of the network, except for its self-excitation (connection bb) and inhibition from ON (connection bo). The difference equation that describes the dynamics of BN in this situation is:

$$BN(k+1) = bb \cdot BN(k) + bo \cdot ON(k) \quad (10)$$

Equation (10) specifies that the state of BN at time step $k+1$ is equal to the sum of its weighted inputs from itself and from ON at time step k . Assuming that it is linear, (i.e., unit states are unbounded), the z -transform of (10) can be taken:

$$z \cdot \overline{BN}(z) - z \cdot BN(0) = bb \cdot \overline{BN}(z) + bo \cdot \overline{ON}(z) \quad (11)$$

where the initial condition $BN(0)$ represents the state of BN at the point when VN and PN initially cut off. Equation (11) can be rearranged to:

$$\overline{BN}(z) = \frac{bo}{(z-bb)} \cdot \overline{ON}(z) + \frac{z}{(z-bb)} \cdot BN(0) \quad (12)$$

where the first and second terms on the right-hand side represent the steady-state response to the constant input from ON , and the transient response to the initial condition $BN(0)$, respectively. Representing $\overline{ON}(z)$ as the z -transform of the unit step $[z/(z-1)]$, and $BN(0)$ as the z -transform of an impulse of size $BN(0)$, the solution of

(12) can be found by the reverse z -transform:

$$BN(k) = \frac{bo}{(1-bb)} + \left(BN(0) - \frac{bo}{(1-bb)} \right) \cdot bb^k \quad (13)$$

Equation (13) describes the BN response after VN and PN both cut off. This equation is undefined for $bb = 1$ (see below).

Equation (13) can be used to define an equilibrium point for BN (Luenberger 1979). When VN and PN are both off, BN is left only with its self-connection (bb), its inhibitory bias connection from ON (bo), and some initial condition $BN(0)$. Equation (13) shows that if the initial state $BN(0)$ is equal to $bo/(1-bb)$, then the second term on the right-hand side will be 0. Since this is the only k -dependent term on the right, $BN(k)$ will remain at $BN(0) = bo/(1-bb)$ for all k . Thus, $BN(0) = bo/(1-bb)$ is an equilibrium point for BN after the burst, with VN and PN both off. Because bo is negative, the equilibrium point will also be negative for $0 \leq bb < 1$. BN could never reach a negative equilibrium point in the nonlinear network, because unit states have a lower bound at 0. However, the equilibrium point will be positive for $bb > 1$, and the equilibrium point decreases as bb increases. For example, the equilibrium point is the absolute value of bo for $bb = 2$, and is half that for $bb = 3$. The equilibrium point is infinite for $bb = 1$.

The negative equilibrium point for $0 \leq bb < 1$ is stable. For $0 \leq bb < 1$, the k -dependent term (second term on the right-hand side) in (13) geometrically decays to 0 as k increases, and thus the state of BN decays to the negative equilibrium point. In contrast, the positive equilibrium point for $bb > 1$ is unstable. For $bb > 1$, the k -dependent term in (13), and thus the state of BN , geometrically rises or falls, to positive or negative infinity, for values of $BN(0)$ that are respectively greater or less than the positive equilibrium point. The existence of the positive equilibrium point limits the amount of direct BN self-excitation, such that bb should be less than $[(BN_{\max} - bo)/BN_{\max}]$ where BN_{\max} is the upper bound on the unit states. In the nonlinear network *with* PN , where bo is -10 and the upper bound is 50 , bb should be less than 1.2 .

An ideal value for the BN self-connection would be 1 , since this would have an infinite (and unattainable) equilibrium point while still providing a substantial amount of positive feedback. Again representing $\overline{ON}(z)$ as the z -transform of the unit step $[z/(z-1)]$, and $BN(0)$ as the z -transform of an impulse of size $BN(0)$, the solution of (12) for the special case of $bb = 1$ can be found by the reverse z -transform:

$$BN(k) = BN(0) + bo \cdot k \quad (14)$$

Equation (14) shows for the special case of $bb = 1$ that, for any negative value of bo , the state of BN will decay linearly with slope bo from any positive initial state $BN(0)$ when VN and PN are both off. It is clear from the linear relationship expressed in (14) that, for the special case of $bb = 1$, the time interval required for the state of BN to decay to 0 increases as $BN(0)$ increases. A similar relationship between decay time to 0 and BN initial state

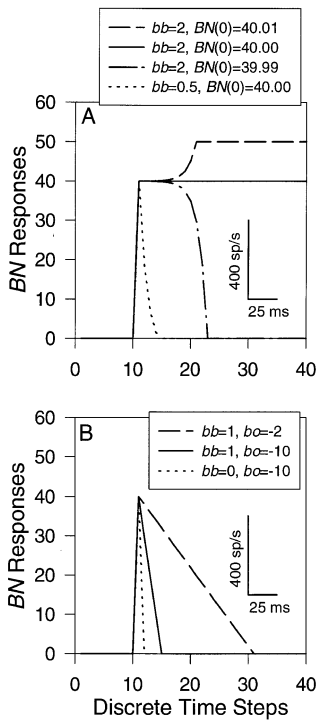


Fig. 6A, B. Burst neuron responses in the nonlinear fast-phase burst-feedback network after the peak of the burst. Unit states are bounded. After the peak of the burst, both the vestibular (VN) and pause (PN) neurons are cut off. This changes the configuration of the network, and the burst neuron (BN) is left only with its self-connection (bb) and with its connection from the ‘on’ neuron (bo) to evolve from its initial condition $[BN(0)]$ at the burst peak. For this reduced network, BN responses for $bb \neq 1$ are described by (13) and shown in **A**. For $bb = 0.5$ (dotted line), the activity of BN will decay geometrically from its initial condition $[BN(0) = 40.00, bo = -2]$. For $bb = 2$, an equilibrium point is reached (continuous line) when $BN(0) = -bo$ (both 40.00 in this case). However, the activity of BN will rise and fall geometrically for values of $BN(0)$ higher and lower than the equilibrium point, respectively $[BN(0) = 40.01, dashed\ line; BN(0) = 39.99, dot-dash\ line; bb = 2$ and $bo = -40$ in both cases]. Also for this reduced network, BN responses for $bb = 1$ are described by (14) and shown in **B**. BN activity will fall linearly with a slope that depends on the value of bo ($bo = -2$, dashed line; $bo = -10$, continuous line). When $bb = 0$ the activity of BN falls immediately in 1 time step (dotted line). $BN(0) = 40$ for all cases shown in **B**

can be demonstrated for $0 \leq bb < 1$ by setting $BN(k) = 0$ in (13) and solving for k . Thus, in the burst-feedback fast-phase network with PN , burst offset duration will be directly proportional to burst amplitude for $bb = 1$, and burst offset duration will increase monotonically with burst amplitude for $0 \leq bb < 1$.

3.7 Burst offset in the nonlinear fast-phase burst-feedback network with the pause neuron

To simulate burst offset responses in the nonlinear network with PN , all connection weights are set to 0 except for the connections to BN from itself (bb) and from ON (bo). This is done to simulate the isolation of BN from the rest of the network that occurs when VN and PN are

both cut off after the peak of the burst. The state of BN is bounded between 0 and 50. Offset responses for various values of bb , bo , and BN initial state $BN(0)$ are shown in Fig. 6. An example of a decay toward an unattainable, negative equilibrium point is shown for $bb = 0.5$ and $BN(0) = 40$ (Fig. 6A, dotted line). The value of $BN(0) = 40$ is approximately that of the burst peak in the network with PN (Fig. 5A). The value of bo is set at -2 to prolong the decay for purposes of illustration. Also shown is an example of a positive equilibrium point for $bb = 2$ and $BN(0) = 40$ (Fig. 6A, continuous line). The value of bo is set at -40 , because the equilibrium point for $bb = 2$ is equal to the absolute value of bo (see above). Slightly increasing or decreasing $BN(0)$ relative to the equilibrium value (40) causes the state of BN to geometrically rise or fall to the upper or lower bound, respectively (Fig. 6A, dashed and dot-dash lines).

An example of linear decay for $bb = 1$ and $bo = -10$ (their values in the network with PN , Table 1C) is shown in Fig. 6B (continuous line). Again $BN(0)$ is set at 40 to approximate the burst peak in the network with PN (Fig. 5A). Decreasing the absolute value of bo decreases the slope of the linear decay (see above) and also prolongs the time that it takes the decay to reach 0, as shown for $bo = -2$ (Fig. 6B, dashed line). Any desired burst offset duration, and a variety of decay profiles (geometric or linear), can be obtained with an appropriate choice of network weights. Observed fast-phase burst offsets have an approximately linear decay and range in duration from 20 to 100 ms (Hikosaka et al. 1977; Curthoys et al. 1981; Markham et al. 1981) The state of BN returns from $BN(0)$ immediately to 0 in 1 time step for $bb = 0$ (Fig. 6B, dotted line). The total duration of a burst with $bb = 0$ would be about 10 ms, and that is unrealistically short. Thus, the analysis demonstrates how burst offset in the model can be controlled by connections to BN from itself (bb) and from ON (bo), and it suggests that the offset of real bursts may also be controlled by the combined effects of burst neuron self-excitation and inhibitory bias.

3.8 Burst amplitude and duration in the nonlinear burst-feedback network with the pause neuron

In the nonlinear network without PN , configured with the weights given in Table 1B, burst amplitude is strongly dependent on input size, while burst duration is independent of input size. These features are unrealistic, but they are eliminated with the inclusion of PN . In the nonlinear network with PN , configured with the weights given in Table 1C, and with the standard input of 0.2, burst amplitude is 868 sp/s (Fig. 5A). When the input is decreased to 0.02 and 0.002, burst amplitude becomes 776 and 791 sp/s, respectively. Burst amplitude saturates at 1000 sp/s when the input is increased to 2.0. Thus, although it does show some relationship to input size, burst amplitude in the network with PN stays within 25% of maximum even as input size (proportional to the slow-phase velocity of nystagmus) varies over 4 orders of magnitude.

In the network without PN each burst, which is the first positive half-cycle of an unstable oscillation, has an

amplitude that is scaled directly with input size. This direct scaling results because the oscillation occurs during the period of linear operation of the network (see above). In contrast, in the network *with PN*, each burst begins with unstable geometric growth during the period when *BN*, *VN*, and *PN* are all on. The geometric growth during this period of linear operation also scales directly with input size. However, unlike the case *without PN*, where the unstable but oscillating state of *BN* will come back to 0 with *VN* still on, in the network *with PN* the unstable but non-oscillating state of *BN* keeps growing until *BN* switches off both *VN* and *PN* and the growth period ends. Because of the constant firing rate of *PN*, the burst amplitude required to switch *PN* off is the same regardless of input size. Also, the burst amplitude required to switch *VN* off depends strongly on the activity level that *VN* must attain to overcome the constant threshold of *BN*, but only weakly on the size of the input that *VN* integrates to reach that threshold. Thus, burst amplitude is largely independent of input size in the network *with PN*.

In these simulations of the network *with PN*, which are deterministic, all bursts will have the same amplitude for the same constant input to *VN*. In another study, a stochastic version of the fast-phase burst-feedback model *with PN* is used to simulate the statistical distribution of inter-fast-phase intervals that are observed during constant-velocity optokinetic nystagmus (Anastasio 1996). The stochastic version is the same as the deterministic version (Fig. 1), except that the input to *VN* is noisy. This causes the response of *VN* to vary stochastically, which in turn causes variability in the inter-burst intervals and burst amplitudes, even though the noisy input has a constant time average. Variability in the inter-burst intervals is due to variability in the times at which the noisy *VN* output brings *BN* to threshold. Also, because the burst continues to grow until *BN* switches *VN* off (see above), variability in *VN* activity causes variability in burst amplitudes in the stochastic version of the model (Anastasio 1996). Noise in other elements of the model could also cause burst amplitudes to vary. However, average burst amplitude would still be largely independent of input size, provided that the average *BN* threshold remains constant.

While burst amplitude in the network *with PN* increases weakly with input size, the time interval between the onset and the peak of the burst decreases weakly with input size. For constant inputs (*IN* states) of 0.002, 0.02, 0.2, and 2.0, the time to peak is about 50, 40, 30, and 20 ms, respectively. The inverse relationship between time to peak and input size results because the geometric growth of the burst scales with the input. Thus, for smaller inputs, the less rapid growth of the burst terminates later because it takes longer for *BN* to reach the amplitude required to switch off *VN* and *PN*.

After the peak of the burst, when *VN* and *PN* are both off, *BN* is left in isolation from the rest of the network, with only the connections from itself (*bb*) and from *ON* (*bo*) remaining. Because $bb = 1$ in the network *with PN*, the burst will decay linearly from the peak with a slope of $bo = -10$, according to (14). The time for the

burst to decay from the peak to 0 is therefore proportional to the amplitude of the burst. The time from peak is about 15, 15, 20, and 25 ms for inputs of 0.002, 0.02, 0.2, and 2.0, respectively. Time from peak is slightly longer for the larger inputs because burst amplitude increases weakly with input size. Overall burst durations for inputs of 0.002, 0.02, 0.2, and 2.0 are 65, 55, 50, and 45 ms, respectively. Because burst amplitude and thus time from peak are largely independent of input size, the weak decrease in overall burst duration as input size increases is due to the decrease in time to peak.

In summary, the nonlinear network *with PN* can generate fast-phase bursts. These bursts have a growth period which is the beginning of an unstable geometric rise that occurs during the brief period of linear operation of the network when *BN*, *VN*, and *PN* are all on. The growth period terminates when the burst amplitude is sufficient for *BN* to switch off both *VN* and *PN*, at which point the burst decays from its peak back to 0. Burst duration decreases weakly as input size increases in the network *with PN*, and this is consistent with the observation that fast-phase duration decreases as slow-phase velocity increases (Honrubia et al. 1971a, b). Also, burst amplitude varies in stochastic versions of the network *with PN*, however, average burst amplitude increases only weakly with input size. Thus, in the network *with PN*, burst duration decreases while burst amplitude increases in roughly the same (small) proportion as input size increases, and this is consistent with the observation that average fast-phase amplitude remains roughly constant as slow-phase velocity increases (Honrubia et al. 1971a, b). The network *with PN* can produce bursts with sufficient amplitude because the *PN* loop augments *BN* positive feedback when it is needed at burst onset, but then opens when *PN* pauses, allowing *BN* to decay under the influence of its own, weaker self-excitation and inhibitory bias. It is possible that this mechanism could account for real fast-phase burst generation during nystagmus.

3.9 Simulations of fast-phase bursts in a distributed burst-feedback network

The real fast-phase burst generator not only produces an intense burst in individual burst neurons, it also produces a burst that is synchronized over an entire population of burst neurons. The positive feedback onto *BN*, which serves to intensify the onset of an individual burst, can also synchronize the burst over the population if the *BN* self-excitation and *PN* loops are shared in a distributed fashion. This is demonstrated by expanding the lumped network *with PN* (Fig. 1) so that there are 10 of each of *BN*, *VN*, and *PN* (there remain only 1 each of *IN* and *ON*).

Each unit in the distributed network sends divergent projections to all units of a given type that are postsynaptic to it, and each of the *BN*, *VN*, and *PN* units receives convergent inputs from all units of a given type that are presynaptic to it, according to the structure of the lumped network (Fig. 1). Connection weights between sets of units are given in Table 1C, but each unit contributes only 10% of the value of that weight. Because synaptic

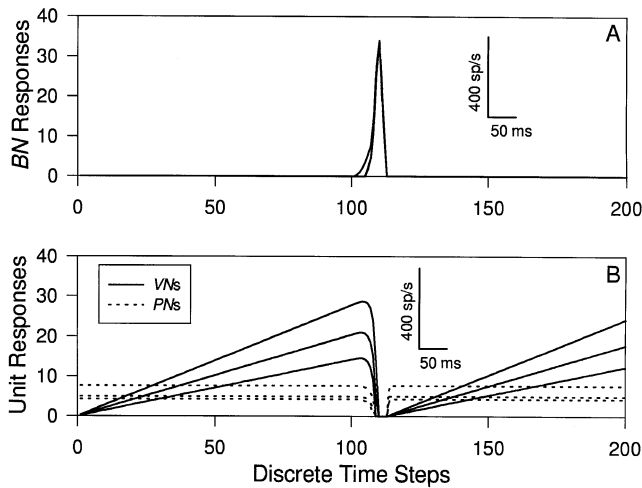


Fig. 7A, B. Neural responses in the distributed, nonlinear fast-phase burst-feedback network *with* pause neurons. Unit states are bounded. The distributed network contains the same types of neurons as the lumped network (Fig. 1), but there are 10 of each of the burst, vestibular, and pause neurons (*BN*, *VN*, and *PN*, respectively). The distributed network produces intense *BN* bursts and complete *VN* and *PN* pauses that are synchronized over the neuronal populations, despite variability in the network connections. Variability in connections causes variability in the responses of the units. The responses of 3 representative *BN* units (*continuous lines*) are shown in **A**, and those of 3 representative *VN* (*continuous lines*) and *PN* (*dotted lines*) units are shown in **B**

weights in the real brainstem are unlikely to be uniform, all weights are randomly perturbed by Gaussian noise with a standard deviation that is 20% of the absolute value of each weight in the distributed network. For example, each of the 10 *BN*s projects to itself and to all 9 of the other *BN*s, and each connection has a weight of 0.1. Each weight is then perturbed by adding to it a number, drawn at random from a standard Gaussian distribution (with mean 0 and standard deviation 1), that is first multiplied by 0.02. All the other connections are similarly distributed and perturbed. Only the *VN* self-connections are not distributed or perturbed, to ensure that the *VNs* act as perfect integrators. The unit states are bounded between 0 and 50 to make the network nonlinear.

In 50% of the randomized versions of the distributed network, intense *BN* bursts and complete *VN* and *PN* pauses are synchronized over the neuronal populations. In the other 50%, synchronized activity does not develop because some *BN*s fail to be activated by the others. This most often results from higher than average inhibition of the *BN*s by *ON*, but synchronized *BN* bursts and *VN* and *PN* pauses can be produced in those networks when the amount of *BN* inhibitory bias is reduced. Variability in connections causes variability in the responses of the units, as shown in Fig. 7, for 3 representative *BN* units (Fig. 7A, continuous lines) and for 3 representative *VN* and *PN* units (Fig. 7B, continuous and dotted lines, respectively). The bursts in all 10 *BN*s are shown in Fig. 8. Some *BN*s begin responding before others, due to stronger input from *VNs*, or lower thresholds due to lower inhibition from *PN*s and/or *ON*. However, *BN* positive

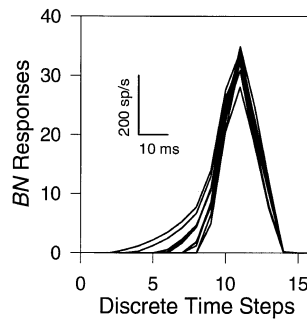


Fig. 8. Burst neuron responses in the distributed, nonlinear fast-phase burst-feedback network *with* pause neurons. Unit states are bounded. The responses of all 10 burst neurons (*BN*s) are shown. These responses vary because of variability in network connections. The spread in lead resembles that observed for long- and medium-lead burst neurons

feedback is complete only when all *BN*s cut on and all *PN*s are beginning to cut off, so the growth period of the burst in some *BN*s starts gradually but then rises more rapidly as the other *BN*s cut on and the *PN*s begin to cut off. The gradual onset of some *BN*s resembles the prelude activity that is observed for some (long-lead) but not other (medium-lead) burst neurons. Variability in real brainstem connections could explain the spread in lead observed during nystagmus for long- and medium-lead burst neurons (Curthoys et al. 1981; Markham et al. 1981).

4 Discussion

The model demonstrates how an intense, temporally circumscribed burst, synchronized over a population, can be generated during nystagmus through feedback at the level of burst neurons. Positive feedback occurs directly from the burst neurons onto themselves and indirectly through the pause neuron loop, and negative feedback occurs through the vestibular nucleus neuron. Positive feedback renders the burst neuron activity unstable, and this instability is what produces the abrupt onset, large amplitude, and synchrony in the population burst. However, the instability does not drive burst neurons into permanent saturation because the burst causes the vestibular and pause neurons to cut off. Vestibular neuron cut-off eliminates the external drive to the burst neuron, while pause neuron cut-off opens the pause neuron loop. This reduces the amount of positive feedback to that provided by burst neuron self-excitation which, if it is not too large, will allow burst neuron activity to decay from its peak back to 0 under the influence of the inhibitory bias input to the burst neuron. Thus, the main function of the pause neuron loop in the fast-phase burst-feedback network is to enhance burst neuron positive feedback transiently, when it is needed at burst onset, by switching on when the burst neuron cuts on and switching off when the pause neuron cuts off. This mechanism of fast-phase burst generation is compatible with experimental findings and with previous models of saccadic burst generation.

4.1 Comparisons of the fast-phase burst-feedback network with neurophysiological data

Brainstem neurons that are involved in the generation of nystagmus include burst, tonic, and pause neurons. The neurophysiological properties of these neural types have been studied primarily in cats and monkeys. Burst neurons are either excitatory or inhibitory, and are located in the reticular formation rostral and caudal to the abducens nuclei, respectively (Shiamzu 1983). The activity of burst neurons has been studied in association with nystagmic fast phases (Hikosaka and Kawakami 1977; Hikosaka et al. 1977; Igusa et al. 1980; Curthoys et al. 1981; Markham et al. 1981; Sasaki and Shimazu 1981) and goal-directed saccades (Luschei and Fuchs 1972; Keller 1974; Kaneko et al. 1981; van Gisbergen et al. 1981; Yoshida et al. 1982; Scudder et al. 1988). Fast-phase and saccadic bursts are similar.

In general, burst amplitude is larger for burst neurons in monkeys than in cats, and larger for inhibitory than for excitatory burst neurons in either animal (Kaneko and Fuchs 1981). Overall, maximum burst amplitude ranges roughly from 400 to 1000 sp/s. *BN* burst amplitudes in the network *with PN* are at the high end of this range. The decay following the burst peak is roughly linear for fast phases. Burst decay in the model is linear for a value of *BN* self-excitation of 1 ($bb = 1$). As the value of *bb* is increased above 1, it becomes increasingly possible that the burst will not decay but will grow after its peak until it saturates at the upper bound where it will remain indefinitely. Real bursts do not exhibit that sort of instability, suggesting that burst neuron self-excitation is similarly limited in the brainstem.

Studies of bursts during goal-directed saccades indicate that burst neurons respond to their input with high gain and then saturate near 1000 sp/s (van Gisbergen et al. 1981). Positive feedback onto *BNs* in the model, both directly and via the *PN* loops, endows *BNs* with high gain until they saturate at 1000 sp/s. Positive feedback could also account for the high gain of real burst neurons. Burst neurons have been classified into long-lead and medium-lead categories, depending upon whether or not they exhibit low-intensity prelude activity prior to the burst. However, burst neurons vary continuously with regard to their prelude activity (lead). Lead varies in the distributed network model due to variability in connection weights. Part of the real spread in lead may similarly result from variability in synaptic connections in the brainstem.

The activity of tonic neurons has been studied during nystagmus (Keller 1974; Hikosaka et al. 1977, 1978; Curthoys et al. 1981; Markham et al. 1981; Nakao et al. 1982) and during other types of eye movements (Luschei and Fuchs 1972; Keller 1974). Tonic units are found in the vestibular nuclei, but are also found in the nucleus prepositus hypoglossi and the reticular formation. During constant nystagmus, tonic neurons show a ramp increase in firing rate during slow-phase eye rotations in their on-direction, and pause abruptly during the ensuing fast phase in their off-direction. Tonic neurons ramp up to rates of about 400 sp/s before they pause, and this sug-

gests that the threshold of burst neurons is exceeded at that point. Tonic neurons are represented by *VN* in the model which ramps up to 400 sp/s and then, in the network *with PN*, pauses abruptly after it brings *BN* to threshold and initiates the burst.

The activity of pause neurons has also been studied in association with nystagmic fast phases (Keller 1974; Curthoys et al. 1981; Markham et al. 1981) and goal-directed saccades (Luschei and Fuchs 1972; Keller 1974, 1977; Evinger et al. 1977, 1982; Strassman et al. 1987). Pause neurons are located in the medial reticular formation. They receive inputs from multiple sources that endow them with a spontaneous firing rate of about 100 sp/s. This nonspecific input is represented by the bias or 'on' unit (*ON*) in the model which provides *PN* with a spontaneous rate of 100 sp/s. The spontaneous rate of real pause neurons slows slightly and then pauses during the burst in burst neurons, and this behavior is reflected by *PN* in the model. Pause lead is intermediate between the leads of long- and medium-lead burst neurons, as in the model. This suggests that long-lead burst neurons begin firing first and then begin to inhibit pause neurons, which in turn disinhibit all burst neurons including medium-lead burst neurons, leading to a synchronized burst and pause throughout the burst and pause neuron populations.

4.2 Compatibility of the fast-phase burst-feedback model with saccade models

Burst generation has been modeled for goal-directed saccades. The eye-position feedback model for saccades (Zee et al. 1976; Zee and Robinson 1979) hypothesized that an efference copy of eye position from the neural integrator is fed back and compared with the goal eye position of the saccade to form an error signal. The saccadic goal is determined by the superior colliculus, but comparison with the efference copy eye-position signal is made directly on burst neurons. In the burst-feedback model for saccades (Scudder 1988), the output of medium-lead burst neurons is fed back to long-lead burst neurons, which then compare the burst-feedback signal with the collicular output and send the error signal forward to the medium-lead burst neurons. In more recent models, the burst neuron output is fed back to the superior colliculus itself (Lefèvre and Galiana 1992; Arai et al. 1994). The burst in these models is generated by the error signal as it drives burst neurons modeled as high-gain elements.

The fast-phase burst-feedback model described here is compatible with these saccade models. To generate saccades, *VN* in the fast-phase burst-feedback model could be replaced by the superior colliculus. *BN* in the model can be driven to threshold by the collicular signal, and the onset of the burst will have high gain due to *BN* self-excitation. Scaling of the burst with the size of the collicular input will be enhanced because the colliculus inhibits *PN* during the burst in the saccade models. The burst will decay after the collicular drive has been eliminated by negative burst feedback and, in addition, the colliculus may actively terminate the burst by exciting

PN which in turn inhibits *BN* (Lefèvre and Galiana 1992).

The saccadic (Scudder 1988) and fast-phase burst-feedback models are structurally similar and display some similarities in behavior. For example, burst decay in both models is approximately linear, and the time interval required for decay from the peak to 0 is proportional to the amplitude of the burst. Also, the pause neuron in both models shows a slight decrease in activity before the pause. However, the structures of the saccadic and fast-phase burst-feedback models differ in certain other respects.

One difference between the burst-feedback models is the way in which long- and medium-lead burst neurons are represented. Both models represent temporally coded long-lead burst neurons that are anatomically co-localized with medium-lead burst neurons and, like them, encode saccade metrics by the temporal characteristics of their bursts (e.g., Hepp and Henn 1983). They do not represent spatially coded long-lead burst neurons, a separate class that are anatomically closer and physiologically more similar to superior colliculus neurons (Hepp and Henn 1983). However, the saccadic burst-feedback model makes a distinction between temporally coded long- and medium-lead burst neurons, in which long-lead project to medium-lead but not vice versa, and long-lead burst neurons have self-excitation but are not part of pause neuron loops while the opposite holds for medium-lead burst neurons. The distributed fast-phase model is more parsimonious in that all *BNs* project to all other *BNs* and to themselves, and all are part of shared *PN* loops. In the distributed fast-phase burst-feedback network, long- and medium-lead burst neurons emerge as a natural consequence of variability in an otherwise common connectivity pattern.

Another structural difference between the burst-feedback models is that the medium-lead burst neuron receives an excitatory bias in the saccadic model (Scudder 1988), but *BN* receives an inhibitory bias in the fast-phase model. As for pause neurons, bias inputs to burst neurons may also arrive from multiple sources. In any case, removal of the pause neuron in the saccadic model causes the medium-lead burst neuron to assume a constant firing rate due to its excitatory bias input. In contrast, *BN* stays off following removal of *PN* in the fast-phase model, due to its inhibitory input from *ON*. However, removal of *PN* in the fast-phase model lowers the threshold on *BN*, and any sustained input above this lowered threshold will cause *BN* to generate a rapid sequence of low-amplitude bursts (as in Fig. 4). Such a sequence could form the basis of pathological oculomotor oscillations. The saccadic eye-position feedback model is also prone to oscillate following removal of the pause neuron (Zee et al. 1976; Zee and Robinson 1979). It has been suggested that the neurophysiological basis of ocular flutter and opsoclonus is oscillation in the saccadic burst generator due to loss of pause neurons, and that the function of pause neurons is to prevent these oscillations by keeping burst neurons off (Zee et al. 1976; Zee and Robinson 1979). *PNs* also help keep *BNs* off in the fast-phase burst-feedback model. However, the main

function of the pause neuron loops in the fast-phase burst-feedback model is to transiently enhance burst neuron self-excitation by closing at burst onset, thereby contributing to the production of an intense burst that is synchronized over the population of burst neurons, but then to open when the pause neurons pause, allowing the burst to terminate.

Acknowledgements. The author wishes to thank Drs. Atlee Jackson, Peter Jung, and Juraj Medanic for consultation and many helpful discussions. He would also like to thank Drs. Attee Jackson, Joseph Malpeli, and Ernst Dow for comments on the manuscript. This work was supported by National Science Foundation grant IBN 92-21823.

References

- Albano JE, Wurtz RH (1982) Deficits in eye position following ablation of monkey superior colliculus, pretectum, and posterior-medial thalamus. *J Neurophysiol* 48:318–337
- Anastasio TJ (1996) A random walk model of fast-phase timing during optokinetic nystagmus. *Biol Cybern* 75:1–9
- Arai K, Keller EL, Edelman JA (1994) Two-dimensional neural network model of the primate saccadic system. *Neural Networks* 7:1115–1135
- Chun K-S, Robinson DA (1978) A model of quick phase generation in the vestibuloocular reflex. *Biol Cybern* 28:209–221
- Curthoys IS, Nakao S, Markham CH (1981) Cat medial pontine reticular neurons related to vestibular nystagmus: firing pattern, location and projection. *Brain Res* 222:75–94
- Curthoys IS, Markham CH, Furuya N (1984) Direct projection of pause neurons to nystagmus-related excitatory burst neurons in the cat pontine reticular formation. *Exp Neurol* 83:414–422
- Evinger C, Kaneko CRS, Johanson GW, Fuchs AF (1977) Omnipause cells in the cat. In: Baker R, Berthoz A (eds) *Control of gaze by brainstem neurons*. Elsevier/North-Holland, New York, pp 337–340
- Evinger C, Kaneko CRS, Fuchs AF (1982) Activity of omnipause neurons in alert cats during saccadic eye movements and visual stimuli. *J Neurophysiol* 47:827–844
- Galiana HL (1991) A nystagmus strategy to linearize the vestibuloocular reflex. *IEEE Trans Biomed Eng* 38:532–543
- Hepp K, Henn V (1983) Spatio-temporal recoding of rapid eye movement signals in the monkey paramedian pontine reticular formation (PPRF). *Exp Brain Res* 52:105–120
- Hikosaka O, Kawakami T (1977) Inhibitory reticular neurons related to the quick phase of vestibular nystagmus: their location and projection. *Exp Brain Res* 27:377–396
- Hikosaka O, Maeda M, Nakao S, Shimazu H, Shinoda Y (1977) Presynaptic impulses in the abducens nucleus and their relation to postsynaptic potentials in motoneurons during vestibular nystagmus. *Exp Brain Res* 27:355–376
- Hikosaka O, Igusa Y, Imai H (1978) Firing pattern of prepositus hypoglossi and adjacent reticular neurons related to vestibular nystagmus in the cat. *Brain Res* 144:395–403
- Honrubia V, Jenkins H, Ward PH (1971a) Computer analysis of optokinetic nystagmus in normal and pathological cats. *Acta Otolaryngol* 80 [Suppl 3]:26–33
- Honrubia V, Katz RD, Strelhoff D, Ward PH (1971b) Computer analysis of induced vestibular nystagmus: rotary stimulation of normal cats. *Acta Otolaryngol* 80 [Suppl 3]:7–25
- Igusa Y, Sasaki S, Shimazu H (1980) Excitatory premotor burst neurons in the cat pontine reticular formation related to the quick phase of vestibular nystagmus. *Brain Res* 182:451–456
- Ito J, Markham CH, Curthoys IS (1984) Projections to eye movement-related pause neuron region in cat using HRP. *Exp Neurol* 86:93–104
- Ito J, Markham CH, Curthoys IS (1986) Direct projection of type II vestibular neurons to eye movement-related pause neurons in the cat pontine reticular formation. *Exp Neurol* 91:331–342
- Kaneko CRS, Fuchs AF (1981) Inhibitory burst neurons in alert trained cats: comparison with excitatory burst neurons and functional

- implications. In: Fuchs A, Baker W (eds) *Progress in oculomotor research*. (Developments in neuroscience, vol 12) Elsevier, New York, pp 63–70
- Kaneko CRS, Evinger C, Fuchs AF (1981) Role of cat pontine burst neurons in generation of saccadic eye movements. *J Neurophysiol* 46:387–408
- Keller EL (1974) Participation of medial pontine reticular formation in eye movement generation in monkey. *J Neurophysiol* 37:316–322
- Keller EL (1977) Control of saccadic eye movements by midline brain stem neurons. In: Baker R, Berthoz A (eds) *Control of gaze by brainstem neurons*. Elsevier/North-Holland, New York, pp 327–336
- King WM, Precht W, Dieringer N (1980) Afferent and efferent connections of cat omnipause neurons. *Exp Brain Res* 38:395–403
- Langer TP, Kaneko CRS (1983) Efferent projections of the cat oculomotor reticular omnipause neuron region: an autoradiographic study. *J Comp Neurol* 217:288–306
- Langer TP, Kaneko CRS (1984) Brainstem afferents to the omnipause region in the cat: a horseradish peroxidase study. *J Comp Neurol* 230:444–458
- Lefèvre P, Galiana HL (1992) Dynamic feedback to the superior colliculus in a neural network model of the gaze control system. *Neural Networks* 5:871–890
- Luenberger DG (1979) *Introduction to dynamic systems*. Wiley, New York
- Luschei ES, Fuchs AF (1972) Activity of brain stem neurons during eye movements of alert monkeys. *J Neurophysiol* 35:445–461
- Markham CH, Nakao S, Curthoys IS (1981) Cat medial pontine neurons in vestibular nystagmus. *Ann NY Acad Sci* 374:189–209
- McCrea RA, Strassman A, May E, Highstein SM (1987) Anatomical and physiological characteristics of vestibular neurons mediating the horizontal vestibulo-ocular reflex of the squirrel monkey. *J Comp Neurol* 264:547–570
- Nakao S, Curthoys IS, Markham CH (1980) Direct inhibitory projection of pause neurons to nystagmus-related pontomedullary reticular burst neurons in the cat. *Exp Brain Res* 40:283–293
- Nakao S, Sasaki S, Schor RH, Shimazu H (1982) Functional organization of premotor neurons in the cat medial vestibular nucleus related to slow and fast phases of nystagmus. *Exp Brain Res* 45:371–385
- Okhi Y, Shimazu H, Suzuki I (1988) Excitatory input to burst neurons from the labyrinth and its mediating pathway in the cat: location and functional characteristics of burster-driving neurons. *Exp Brain Res* 72:457–472
- Robinson DA (1989) Control of eye movements. In: Brooks VB (ed) *Handbook of physiology*, sect 1: The nervous system, vol II, part 2. American Physiology Society, Bethesda, pp 1275–1320
- Sasaki S, Shimazu H (1981) Reticulo-vestibular organization participating in generation of horizontal fast eye movement. *Ann NY Acad Sci* 374:130–143
- Schiller PH, True SD, Conway JL (1980) Deficits in eye movements following frontal eye-field and superior colliculus ablations. *J Neurophysiol* 44:1175–1189
- Schmid R, Lardini F (1976) On the predominance of anti-compensatory eye movements in vestibular nystagmus. *Biol Cybern* 23:135–148
- Scudder CA (1988) A new local feedback model of the saccadic burst generator. *J Neurophysiol* 59:1455–1475
- Scudder CA, Fuchs AF, Langer TP (1988) Characteristics and functional identification of saccadic inhibitory burst neurons in the alert monkey. *J Neurophysiol* 59:1430–1454
- Shimazu H (1983) Neuronal organization of the premotor system controlling horizontal conjugate eye movements and vestibular nystagmus. In: Desmedt JE (ed) *Motor control mechanisms in health and disease*. Raven Press, New York, pp 565–588
- Strassman A, Highstein SM, McCrea RA (1986a) Anatomy and physiology of saccadic burst neurons in the alert squirrel monkey. I. Excitatory burst neurons. *J Comp Neurol* 249:337–357
- Strassman A, Highstein SM, McCrea RA (1986b) Anatomy and physiology of saccadic burst neurons in the alert squirrel monkey. II. Inhibitory burst neurons. *J Comp Neurol* 249:358–380
- Strassman A, Evinger C, McCrea RA, Baker RG, Highstein SM (1987) Anatomy and physiology of intracellularly labeled omnipause neurons in the cat and squirrel monkey. *Exp Brain Res* 67:436–440
- van Gisbergen JAM, Robinson DA, Gielen S (1981) A quantitative analysis of generation of saccadic eye movements by burst neurons. *J Neurophysiol* 45:417–442
- Yoshida K, McCrea R, Berthoz A, Vidal PP (1982) Morphological and physiological characteristics of inhibitory burst neurons controlling horizontal rapid eye movements in the alert cat. *J Neurophysiol* 48:761–784
- Zee DS, Robinson DA (1979) A hypothetical explanation of saccadic oscillations. *Ann Neurol* 5:405–414
- Zee DS, Optican LM, Cook JD, Robinson DA, Engel WK (1976) Slow saccades in spinocerebellar degeneration. *Arch Neurol* 33:243–251